Acta Biochim Biophys Sin 2023, 55(11): 1758–1769
https://doi.org/10.3724/abbs.2023236
Advance Access Publication Date: 8 October 2023
Original Article

Original Article

A novel ferroptosis-related microRNA signature with prognostic value in osteosarcoma

Jie Shao[1,†], Yi Zhang[1,†], Zhu Chang[2,†], Shiyao Du[2], Wei Li[1], Yushu Bai[1,*], Chunwen Lu[2,*], and Tianming Xu[2,*]

[1]Department of Spine Surgery, Changhai Hospital, Naval Medical University (Second Military Medical University), Shanghai 200043, China, and [2]Department of Orthopaedic Surgery, Naval Medical University (Second Military Medical University), Shanghai 200052, China
[†]These authors contributed equally to this work.
*Correspondence address. Tel: +86-15721570948; E-mail: xutm_smmu@126.com (T.X.) / Tel: +86-13671582638; E-mail: luchunwench@163.com (C.L.) / Tel: +86-13764549997; E-mail: spinebaiys@163.com (Y.B.)

Received 20 February 2023 Accepted 6 May 2023

Abstract

The induction of ferroptosis is suggested to be a potential therapeutic strategy for cancers. MicroRNAs (miRNAs) are reported to play an important role in cell death processes. This study aims to construct and validate a risk model based on ferroptosis-related miRNAs (FR_miRNAs) to predict prognosis and identify novel therapeutic targets for osteosarcoma. Data from the Therapeutically Applicable Research to Generate Effective Treatments database are used as the training cohort. A prognostic signature based on two FR_miRNAs (miR-635 and miR-593) is developed using univariate Cox regression, least absolute shrinkage and selection operator regression, and multivariate Cox regression analyses. The area under the curve values of the prognostic signature to predict the 1-year, 2-year, 3-year, and 5-year overall survival rates in patients with osteosarcoma are 0.782, 0.781, 0.722, and 0.777, respectively, indicating a good predictive ability. Based on the risk score, patients are divided into low-risk and high-risk groups. Patients with high-risk scores are associated with poor survival. The risk level is determined to be an independent prognostic factor. A nomogram is established for predicting prognosis. The expression levels of *PRNP* (miR-635-related ferroptosis-related gene (FRG); $P=0.024$) and *HILPDA* (miR-593-related FRG; $P=0.025$) are significantly different between the low-risk and high-risk groups. All results are validated in an external cohort (GSE39040). The results of the functional assay reveal that miR-635 mimics inhibit osteosarcoma (OS) cell proliferation and migration, whereas miR-593 overexpression exerts the opposite effect. In conclusion, miR-635 and miR-593 exert contrasting regulatory effects on OS cell proliferation and migration.

Key words osteosarcoma, ferroptosis-related miRNA, prognostic gene signature, miR-635, miR-593

Introduction

Osteosarcoma (OS), which is the most common bone tumor, is derived from bone marrow mesenchymal stem cells (BMSCs) [1]. The annual incidence of OS in children and adolescents is 1–3 cases per million individuals [2]. The long bones of limbs are highly susceptible to developing OS [3]. A multi-agent chemotherapy regimen significantly improves the prognosis of localized OS and has increased the five-year overall survival rate from $<20\%$ to 65%–70% [4]. However, the long-term survival of patients with OS is poor, especially in those with recurrent and metastatic OS. The genome of OS is highly unstable with frequent aneuploidy presentations. Additionally, OS exhibits heterogeneity within and between individuals. Thus, the identification of effective therapeutic targets for OS is challenging [2,5]. To predict the prognosis of patients with OS, there is an urgent need to identify biological pathways and effective biomarkers.

In the last few decades, the discovery of regulated cell death (RCD) pathways has markedly contributed to improving tumor treatment [6]. Ferroptosis, a novel type of RCD mediated by the pathological accumulation of reactive oxygen species, has piqued the interest of oncologists [7]. Several studies have demonstrated the potential therapeutic value of ferroptosis in various cancers,

© The Author(s) 2023. This is an open access article distributed under the terms of the Creative Commons Attribution-NonCommercial-NoDerivs License (https://creativecommons.org/licenses/by-nc-nd/4.0/).

such as lung and breast cancers [8,9]. Ferroptosis-related genes (FRGs) were subsequently identified as new therapeutic targets with prognostic value in OS [10,11]. Furthermore, ferroptosis can be triggered in OS cells, inhibiting the growth and development of OS [12]. These findings have provided the theoretical foundation for oncologists to confirm ferroptosis activation as a novel and potential therapeutic approach for OS.

Non-coding RNAs (ncRNAs), such as microRNAs (miRNAs), are reported to be potential therapeutic targets for various diseases, including cancer [13]. miRNAs are small and highly conserved single-stranded ncRNAs with a length of 17–25 nucleotides [14]. Additionally, miRNAs mediate diverse fundamental biological processes, including the occurrence and development of cancers, by regulating gene transcription [13,15]. Phase II or III clinical trials of drugs targeting miRNAs are currently ongoing [14]. Previous studies have examined the correlation between OS and miRNAs. For example, one study reported that several miRNAs (such as miR-223 and miR-224-3p) can interact with mRNAs or lncRNAs and regulate the malignant behaviors of OS, including cancer cell proliferation, invasion, and drug resistance [16]. Furthermore, metastasis is the major hallmark of the advanced development of OS. The mechanisms underlying OS metastasis are complex. miRNAs are reported to be involved in several signaling pathways that inhibit OS metastasis. Clinical trials on drugs that target miRNAs to treat OS are ongoing [17]. Therefore, the foundation of treating OS by targeting miRNAs is available. Moreover, the correlation between miRNAs and ferroptosis, which are novel therapeutic targets, has been examined in some cancers. For example, miR-522 suppresses ferroptosis and promotes chemoresistance in gastric cancer [18]. To the best of our knowledge, although FRGs have been previously identified in patients with OS [10,11], limited studies have focused on the correlation between miRNAs and ferroptosis, as well as the prognostic value of ferroptosis-related miRNAs (FR_miRNAs) in the progression of OS.

This study aimed to construct and validate a prognostic signature based on FR_miRNAs for patients with OS. Additionally, bioassays were performed to further explore the role of FR_miRNAs in OS.

Materials and Methods

Data collection and screening

The transcriptome sequencing data and relative clinical information of 101 patients with OS were retrieved from the Therapeutically Applicable Research to Generate Effective Treatments (TARGET) database. The inclusion criteria were as follows: (1) unduplicated samples; (2) samples with active follow-up and confirmed survival status data; and (3) samples of patients whose survival duration was >0 months. Additionally, the GSE39040 dataset was downloaded from the Gene Expression Omnibus (GEO) database and used as the external validation cohort. The transcript kilobase per million values were generated for normalization in the training cohort. Meanwhile, the data in the validation cohort were normalized using the R package "limma". FRGs were obtained from the Human Gene Database (https://www.genecards.org) by searching the keyword "ferroptosis", as well as from previous literature.

Identification of miRNAs associated with ferroptosis

The total numbers of FRGs and miRNAs identified in this study were 111 and 1301 (Supplementary Tables S1 and S2), respectively. Univariate Cox regression analysis was performed to identify FRGs associated with the prognosis of patients with OS. FRGs with $P<0.05$ were screened as candidate genes. Next, the correlation between miRNAs and candidate genes was examined using Pearson's correlation test. miRNAs with $|\text{Pearson coefficient}|>0.4$ and $P<0.001$ were used for further analyses [19–21].

Development and evaluation of a prognostic signature based on FR_miRNAs

To construct the optimal prognostic signature, FR_miRNAs were subjected to univariate Cox regression analysis, followed by least absolute shrinkage and selection operator (LASSO) regression and multivariate Cox regression analysis. Only FR_miRNAs with $P<0.05$ in univariate Cox regression analysis were subjected to subsequent LASSO and multivariate Cox regression analyses to develop the prognostic signature. The risk score for each patient was calculated as follows:

$$Risk\ score=\sum_{i}^{n}(Coefficient_{FR_miRNAs}\times Expression_{FR_miRNAs})$$

Based on the optimal cutoff value of the risk score, 95 patients with OS were categorized into low-risk and high-risk groups. The log-rank test was used to compare the survival curves of the high-risk and low-risk groups. Additionally, the risk score of each sample was reordered, and the risk curve and survival status-related scatterplot are shown together with the heatmap of FR_miRNA expression. The accuracy of this signature was assessed using the area under the receiver operating characteristic (ROC) curve (AUC) values. For the validation process, each individual in the GEO dataset was assigned a risk score based on the same formula and coefficients derived from the training cohort, which resulted in the stratification of all samples into two risk groups. Kaplan–Meier (KM) and ROC curves, survival-related scatterplots, and heatmaps were generated for the two subgroups. All analyses were performed using the "survminer", "survival", and "survivalROC" R packages.

Development of a nomogram based on the "risk score" and clinical factors

The "risk score", which was defined as a binary variable (low-risk/high-risk group), was subjected to univariate and multivariate Cox regression analyses with other clinical variables (age, sex, and metastatic status) to develop a prognostic nomogram. Components with $P<0.05$ were used to develop a nomogram to predict the individual survival probability of patients with OS. The nomogram was constructed using the R package "rms". The accuracy of the nomogram was assessed using ROC and calibration curves. Additionally, the effect of the risk levels on the prognosis of patients in distinct clinical variable groups was examined using the log-rank test.

Cell culture and transfection

The cell line human bone marrow-derived mesenchymal stem cells (BMSCs) and OS cell line HOS were both obtained from the National Collection of Authenticated Cell Cultures (Shanghai, China). BMSCs were cultured in MEM Alpha Modification (HyClone, Logan, USA), while HOS were cultured in DMEM (Gibco, Grand Island, USA). All media were supplemented with 10% (v/v) fetal bovine serum (Gibco) and 1% (v/v) penicillin-streptomycin.

The miRNA mimics transfection was performed using the

lipofectamine 3000 (Invitrogen, Carlsbad, USA) according to the manufacturer's instructions when the cells were at an appropriate confluency per well (60%–70%) in a 6-well plate. The sequence of two miRNA mimics and the negative control were as the following: miR-635 mimics: 5′-ACUUGGGCACUGAAACAAUGUCC-3′; miR-593-3p mimics: 5′-UGUCUCUGCUGGGGUUUCU-3′; negative control mimics: 5′-UUUGUACUACACAAAAGUACUG-3′. The oligo sequences were synthesized by Shanghai Zorin Biological Technology Co., Ltd (Shanghai, China).

Quantitative real-time polymerase chain reaction (qRT-PCR)

The expression levels of miR-635 and miR-593 in BMSCs and the OS cell line HOS were examined using qRT-PCR method. The whole process of qRT–PCR was performed using a commercial kit (Accurate Biology, Changsha, China) following the manufacturer's instructions, including extracting total RNA, reverse transcription PCR and quantitative real-time PCR. The results were calculated by the $2^{-\Delta\Delta Ct}$ method. The primer sequences were as follows: miR-635, 5′-CATTGTTTTGTGTCCATTGAGCT-3′ (forward) and 5′-AGTGCAGGGTCCGAGGTATT-3′ (reverse); miR-593-3p, 5′-CGCGTGTCTCTGCTGGG-3′ (forward) and 5′-AGTGCAGGGTCCGAGGTATT-3′ (reverse).

Cell viability and migration assay

Cell viability was evaluated using the cell counting kit-8 (CCK-8) assay (Dojindo Laboratories, Rockville, USA) following the manufacturer's instructions. Briefly, the cells were seeded in a 96-well plate at a density of 5×10^3 cells/well and cultured for the indicated durations. Next, the cells were incubated with CCK-8 reagent (10 μL/well) for 2 h at 37°C. The absorbance of the reaction mixture was measured at 450 nm with three duplicates.

Transwell assays were performed using Boyden chambers (Corning, Steuben County, USA). Briefly, 1×10^5 cells (200 μL) were cultured with 1% fetal bovine serum (FBS) in the upper chamber. The lower chamber was filled with 500 μL of medium supplemented with 10% FBS. After 18 h of culture, the cells were fixed in 4% paraformaldehyde and stained with 0.1% crystal violet. The cells on the upper surface were removed, and the number of migrated cells was counted in three random visual fields using Image-Pro Plus 6.0 (Media Cybernetics, Silver Spring, USA).

Statistical analysis

All statistical analyses were performed using R (version 4.0.1; https://www.r-project.org) and GraphPad Prism 8.0. Quantitative data are presented as the mean ± standard deviation and/or range, whereas categorical variables are presented as counts and percentages. KM survival curves were compared using the log-rank test. Candidate FR miRNAs used to develop the signature were selected using univariate Cox regression, LASSO regression, and multivariate Cox regression analyses. Quantitative variables were compared using Student's *t*-test, while categorical variables were compared using the chi-square test. All statistical tests were two-tailed unless specified otherwise. Differences were considered significant at $P < 0.05$.

Results

Screening of candidate FR_miRNAs

Based on the inclusion criteria, data from 95 samples from the TARGET database were included in this study as the training set. Univariate Cox regression analysis revealed that 20 FRGs (15 protective FRGs and 5 risk FRGs) were associated with the prognosis of patients with OS (Figure 1A). Next, 17 miRNAs were screened as potential FR_miRNAs based on the selection standards using Pearson's correlation tests (Figure 1B and Table 1).

Construction of the FR_miRNA-based signature in the training cohort

To enhance the accuracy of the prognostic model, univariate Cox regression analysis was performed to identify the prognosis-related FR_miRNAs among the 17 candidate FR_miRNAs. miR-210, miR-593, miR-3687, and miR-4664 were identified as risk miRNAs for the survival of patients with OS, whereas miR-635 and miR-4482.1 were identified as protective miRNAs (Figure 2A). Additionally, cross-validation was performed using LASSO regression analysis (Figure 2B,C). Finally, miR-635 and miR-593 (both $P < 0.001$) were used to construct the prognostic signature (Figure 2D). The hazard ratio (HR) values of miR-635 and miR-593 were 0.526 (confidence interval (CI): 0.379–0.729) and 1.963 (CI: 1.411–2.731), respectively. The best cutoff value was 1.52196. Patients were further categorized into high-risk and low-risk groups. The KM survival curve revealed that the overall survival rate of the low-risk group was higher than that of the high-risk group ($P < 0.001$; Figure 3A). The risk curve and survival status-related scatterplot also revealed

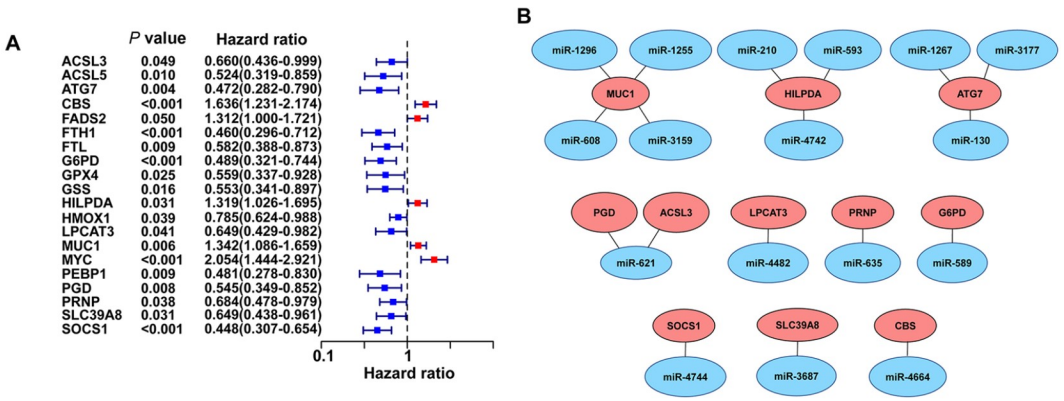


Figure 1. Selection of candidate ferroptosis-related microRNAs (FR_miRNAs) (A) Univariate Cox regression analysis of FRGs associated with the prognosis of patients with osteosarcoma. (B) FR_miRNAs correlated with selected FRGs.

similar prognostic outcomes for the two groups (Figure 3B,C). Furthermore, miR-635 and miR-593 were mainly expressed in patients with low and high risk scores, respectively (Figure 3D). This suggests that miR-635 was associated with improved prognosis, whereas miR-593 was associated with poor prognosis. The results of the log-rank tests demonstrated that miR-635 ($P < 0.001$) and miR-593 ($P = 0.0012$) were significant prognostic factors for patients with OS (Figure 3E,F), which was consistent with the assumptions in Figure 3D. The developed signature exhibited good performance in predicting the prognosis of patients with OS. The AUC values for 1-year, 2-year, 3-year, and 5-year overall survival rates were 0.782, 0.781, 0.722, and 0.777, respectively (Figure 3G).

Table 1. The results of the analysis of the correlation between FRGs and miRNAs

FRG	miRNA	Correlation index	*P*-value
HILPDA	miR-210	0.546385301	1.02E−08
MUC1	miR-608	0.448140719	5.26E−06
PRNP	miR-635	0.47635856	1.06E−06
HILPDA	miR-593	0.425478537	1.72E−05
ACSL3	miR-621	0.450778701	4.56E−06
PGD	miR-621	0.415082249	2.88E−05
ATG7	miR-130	0.541498956	1.46E−08
G6PD	miR-589	0.411636307	3.41E−05
MUC1	miR-1296	0.401651644	5.48E−05
MUC1	miR-1255	0.401159016	5.61E−05
ATG7	miR-1267	0.442940991	6.96E−06
SOCS1	miR-4744	0.439091347	8.53E−06
SLC39A8	miR-3687	−0.44164998	7.45E−06
MUC1	miR-3159	0.415997719	2.76E−05
ATG7	miR-3117	0.402891815	5.17E−05
CBS	miR-4664	0.412285479	3.30E−05
HILPDA	miR-4742	0.497998784	2.82E−07
LPCAT3	miR-4482	0.423749447	1.88E−05

Risk level is an independent factor for OS

Next, univariate and multivariate Cox regression analyses were performed to determine the independent prognostic factors by incorporating risk level (low-risk/high-risk groups), age (≤19/ >19 years), gender (male/female), and metastatic status (non-metastasis/metastasis). As shown in Table 2, the risk level (HR: 4.544; 95% CI: 2.281–9.053; $P < 0.001$) and metastatic status (HR: 4.599; 95% CI: 2.307–9.166; $P < 0.001$) were associated with the OS of patients (Figure 4A,B). Next, a nomogram based on the risk level and metastatic status was constructed to predict the 1-year, 2-year,

Table 2. Multivariate Cox regression analysis of clinical variables associated with the overall survival rate

Variable	HR	CI_95%L	CI_95%H	*P*-value
Age	1.1638141	0.4758023	2.8466932	0.7395748
Gender	1.5179273	0.7585927	3.0373391	0.2382915
Metastasis	4.5987357	2.3073322	9.1657239	1.45E−05
Risk level	4.5440887	2.2808444	9.0531129	1.67E−05

HR, hazard ratio; CI, confidence interval; L, lower limit; H, upper limit.

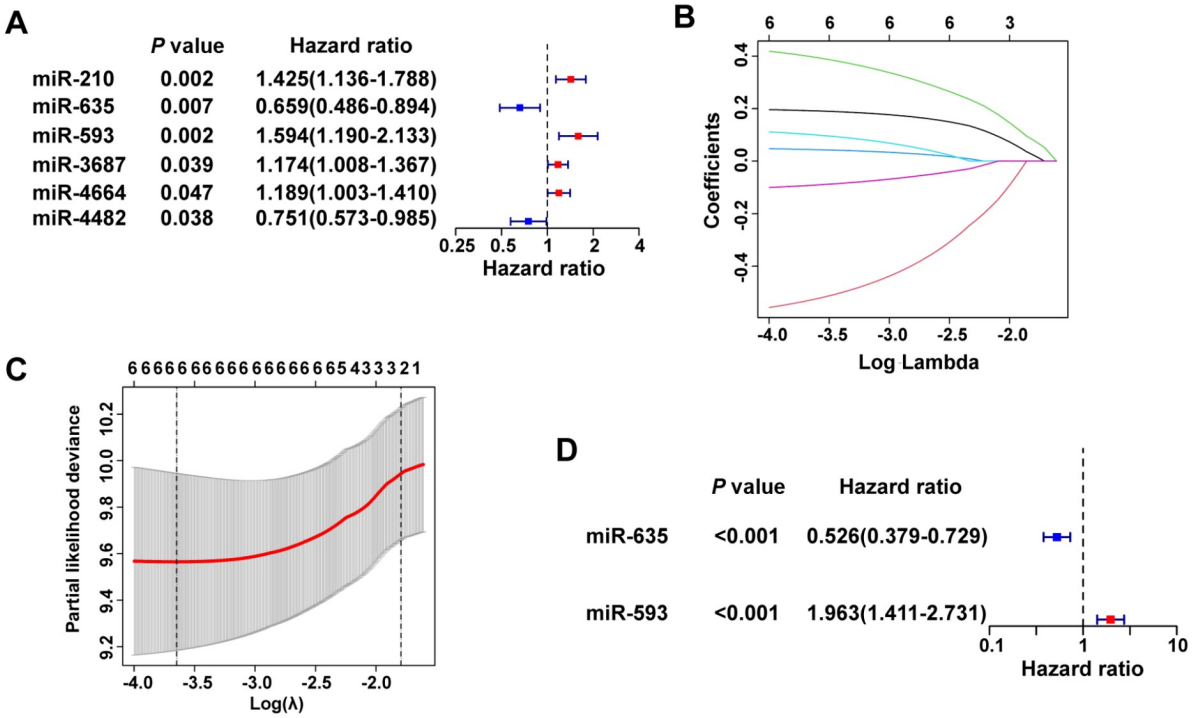


Figure 2. Selection of optimal FR_miRNAs to develop a prognostic signature (A) Univariate Cox regression analysis of candidate FR_miRNAs associated with the prognosis of patients with osteosarcoma. (B) LASSO regression analysis of six FR_miRNAs. (C) Cross-validation using LASSO regression analysis. (D) Selection of two optimal FR_miRNAs after multivariate Cox regression analysis.

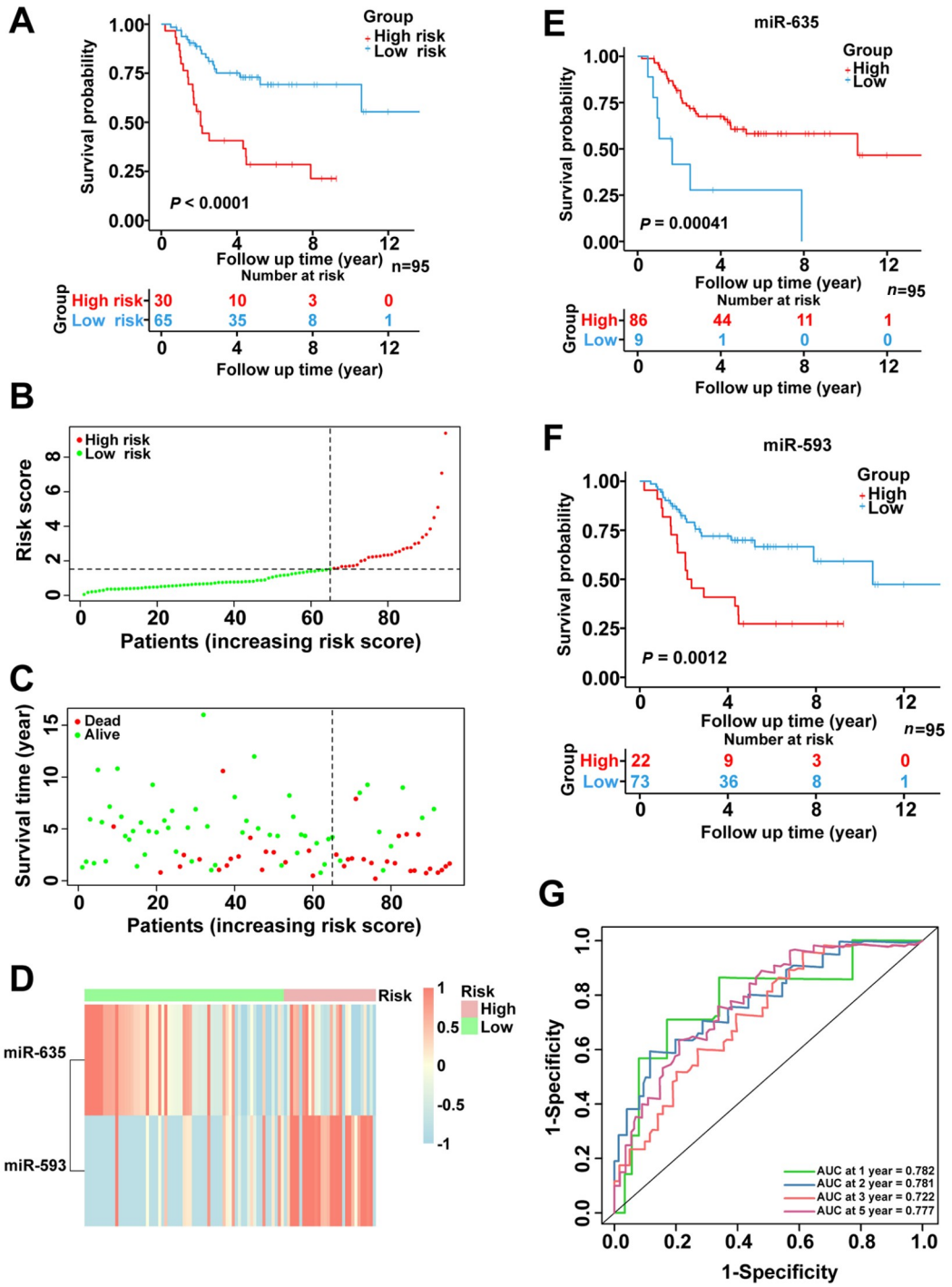


Figure 3. Construction of a prognostic model based on two FR_miRNAs in the training cohort (A) Survival status of the two risk groups was compared using the log-rank test. (B) Distribution of risk score of patients in the two risk groups. (C) Distribution of overall survival status of patients in the two risk groups. (D) Differential expression of two FR_miRNAs between the low-risk and high-risk groups. (E) Kaplan-Meier (KM) survival curve according to miR-635 expression. (F) KM survival curve according to miR-593 expression. (G) ROC curve with the area under the ROC curve values for 1-year, 2-year, 3-year, and 5-year survival rates to assess the predictive ability of the prognostic model.

and 3-year OS rates (Figure 4C). As shown in Figure 4D, the ROC curve revealed satisfactory accuracy. The AUC values for the 1-year, 2-year, and 3-year survival rates were 0.911, 0.811, and 0.751, respectively. Furthermore, the predicted and observed outcomes were consistent in the calibration plots (Figure 4E–G).

Additionally, the prognosis of patients in the low-risk and high-risk groups based on distinct clinical variables was analyzed (Table 3). Age, gender, and metastatic status were not significant factors affecting the risk level of patients with OS (Supplementary Table S3). However, the survival probabilities of patients with high risk scores were lower than those of patients with low risk scores in all distinct clinical variable subgroups (Figure 5A–F). The expression

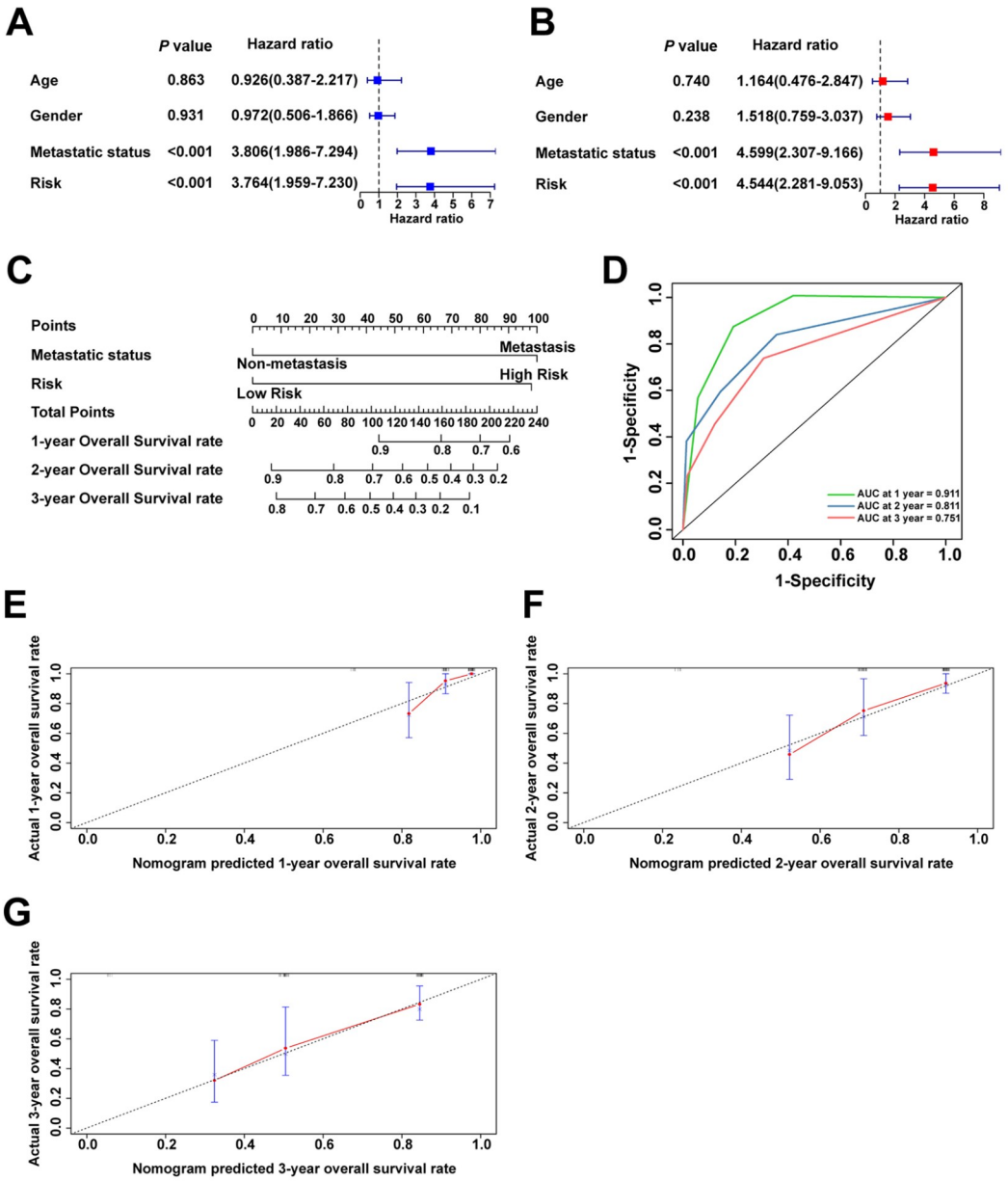


Figure 4. Construction and evaluation of a nomogram to assess the survival probabilities of patients with osteosarcoma (A) Results of univariate Cox regression analysis performed by combining the risk level with other clinical variables. (B) Results of multivariate Cox regression analysis performed by combining the risk level with other clinical variables. (C) Construction of a nomogram based on two variables to predict the survival probabilities of patients with osteosarcoma. (D) ROC curve with the area under the ROC curve values for 1-year, 2-year, and 3-year survival rates to assess the predictive ability of the nomogram. (E–G) Calibration plots for the 1-year, 2-year, and 3-year survival rates to test the performance of the newly established nomogram.

levels of PRNP (miR-635-associated FRG; $P=0.024$) and HILPDA (miR-593-associated FRG; $P=0.025$) in patients with low risk scores were significantly lower than those in patients with high risk scores (Figure 6A,B). These findings were consistent with the data shown in Figure 1A. Other FRGs exhibiting significant differential expression between the risk groups were *GSS* ($P=0.019$), *LPCAT3* ($P=0.047$), *MUC1* ($P=0.024$), and *SOCS1* ($P=0.025$) (Figure 6C–F). In contrast, the expression levels of *ACSL3* ($P=0.21$), *ACSL5* ($P=0.28$), *ATG7* ($P=0.71$), *CBS* ($P=0.78$), *FADS2* ($P=0.78$), *FTH1* ($P=0.61$), *FTL* ($P=0.84$), *G6PD* ($P=0.29$), *GPX4* ($P=0.62$), *HMOX1* ($P=0.67$), *MYC* ($P=0.20$), *PEBP1* ($P=0.26$), *PGD* ($P=0.91$), and *SLC39A8* ($P=0.77$) were not significantly different between the risk groups (Supplementary Figure S1).

External validation of the FR_miRNA signature

The GSE39040 dataset, comprising data from 65 OS samples, was used as the validation cohort. According to the algorithm in the training set, patients in the validation cohort were divided into two risk groups based on the optimal cutoff value of the risk score. The overall survival rates of patients with high risk scores were markedly lower than those of patients with low risk scores ($P=0.011$; Figure 7A), which was consistent with the distribution

Table 3. Multivariate Cox regression analysis of clinical variables associated with the overall survival rate

Factor		Factor		*P*-value
		High (*n*/%)	Low (*n*/%)	
Gender	Female	15 (50.0)	25 (38.5)	0.404
	Male	15 (50.0)	40 (61.5)	
Age (years)	≤19	25 (83.3)	53 (81.5)	1.000
	>19	5 (16.7)	12 (18.5)	
Metastasis	Non-metastasis	21 (70.0)	51 (78.5)	0.524
	Metastasis	9 (30.0)	14 (21.5)	

HR, hazard ratio; CI, confidence interval; L, lower limit; H, upper limit.

of risk scores (Figure 7B,C). Moreover, the expression patterns of miR-635 and miR-593 varied between the two risk groups, which was consistent with the training cohort analysis results (Figure 7D). The upregulated expression of miR-635 was correlated with good prognosis, whereas the downregulated expression of miR-593 was correlated with improved prognosis (Figure 7E,F). The AUC values for the 1-year, 2-year, 3-year, and 5-year OS rates in the validation cohort were 0.684, 0.633, 0.668, and 0.633, respectively (Figure 7G).

miR-635 and miR-593 regulate OS cell proliferation and migration

Next, the roles of miR-635 and miR-593 in the malignant behaviors of OS were examined. First, the miRNA expression levels in healthy

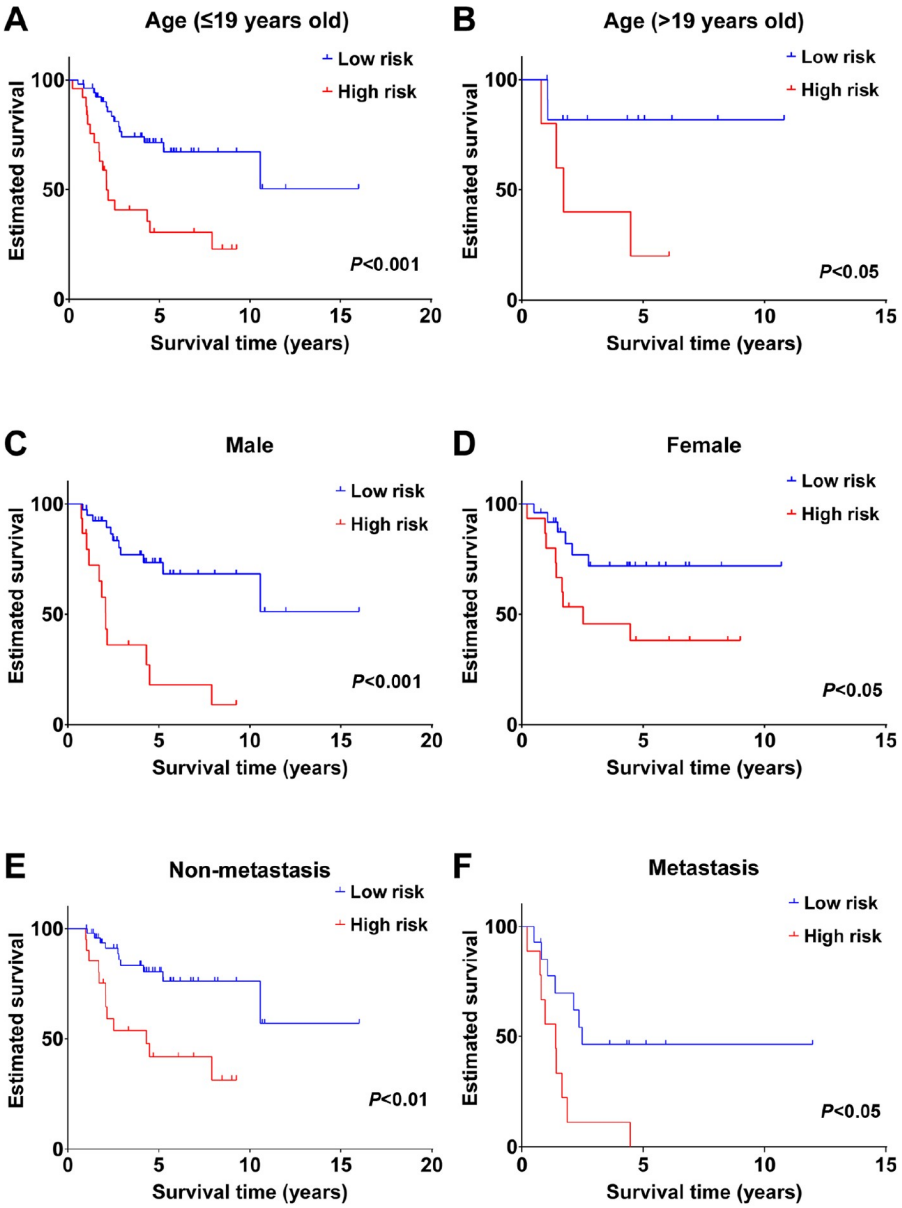


Figure 5. Identification of risk level as an independent prognostic factor in patients with osteosarcoma (A,B) The overall survival rate of patients in the two risk groups according to age. (C,D) The overall survival status of patients with low and high risk scores according to gender. (E,F) KM survival curves of risk groups according to metastatic status.

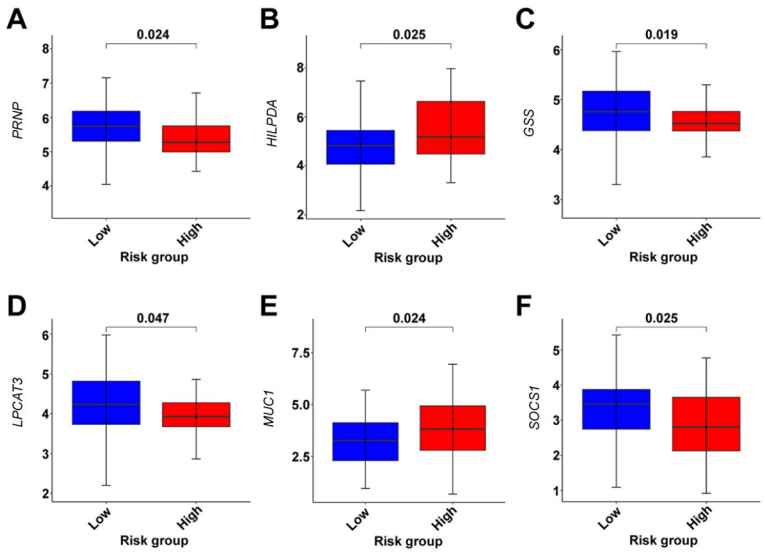


Figure 6. Comparative analysis of the mRNA expression levels of significant FRGs between the high-risk and low-risk groups (A–F) The *PRNP*, *HILPDA*, *GSS*, *LPCAT3*, *MUC1*, and *SOCS1* mRNA levels in the two risk groups.

BMSCs and the OS cell line HOS were examined. Consistent with our previous findings, compared with those in BMSCs, miR-635 expression was downregulated and miR-593 expression was upregulated in OS cells (Figure 8A). Transfection with miR-635 mimics inhibited OS cell proliferation and migration, whereas transfection with miR-593 overexpression constructs promoted OS cell proliferation and migration (Figure 8B,C). Thus, *in vitro* experiments demonstrated the protective effects of miR-635 and the adverse effects of miR-593 in OS.

Discussion

Several studies have reported that ferroptosis activation is a potential therapeutic strategy to suppress the development of cancer [22]. In contrast to other RCD processes, ferroptosis is associated with distinct cellular morphology, molecular pathways, and gene expression profiles [7]. Ferroptosis can be induced through intrinsic (via GPX4) or extrinsic pathways (via serotransferrin/lactotransferrin) [6,7,23,24]. Various drugs, such as sorafenib and withaferin A, have been developed to target ferroptosis-related pathways in oncology. Sorafenib was reported to suppress OS growth, angiogenesis, and metastasis [25]. In phase II clinical trials, withaferin A was demonstrated to exert therapeutic effects on OS and breast cancer [6]. The discovery of miRNAs has provided oncologists with novel insights for treating cancers [26]. Alterations in miRNAs and their biogenesis machinery were reported to be etiological factors for cancers [27]. The tumor microenvironment plays a crucial role in regulating miRNA biogenesis, methylation, and transcriptional changes and consequently modulating miRNA levels in cancer cells. The dysregulation of miRNAs or their biogenesis is associated with poor survival outcomes in several cancer types [28]. As miRNAs function as oncogenes (oncomiRs) or tumor suppressors, novel cancer therapeutic methods can be developed using miRNA mimics or molecules that target miRNAs (antimiRs) [14]. For example, miR-155 is associated with the development of lymphoma and functions as an oncomiR in several types of solid tumors [29–32]. Meanwhile, miR-16 is downregulated in some solid tumors, such as melanoma, colon cancer, and bladder cancer [33,34]. Clinical trials on several miRNA mimics or antimiRs are currently ongoing. Targeting miRNAs is a promising therapeutic approach for cancers.

This study demonstrated that miR-635 is a protective FR_miRNA by using the prognostic model. miR-635 was reported to function as a tumor suppressor in several tumors. Additionally, miR-635 significantly inhibits the tumorigenesis of non-small cell lung cancer by downregulating the expression of endogenous YY1, a zinc finger protein that is upregulated in various cancers [35]. The expression of miR-635 in OS tissues is downregulated compared with that in non-tumorous tissues [36]. miR-635 inhibits the proliferation and invasion of OS cells *in vitro* [36], which is consistent with the results of the cell viability and migration assays in this study (Figure 8B,C). LncRNA DUXAP8 promotes the development of OS by upregulating the expression of TOP2A. However, miR-635 mitigates the DUXAP8-induced upregulation of TOP2A [37]. Thus, miR-635 exerts protective effects in patients with OS.

miR-593, which was demonstrated to be a risk FR_miRNA, is associated with poor outcomes in patients with OS. To the best of our knowledge, the role of miR-593 in cancer development remains controversial. Some studies proposed that miR-593 functions as an oncomiR and affects the AMP-activated protein kinase signaling pathway and epithelial-mesenchymal transition process by targeting ADIPOR1, which promotes the malignant behaviors of prostate cancer cells, such as cancer cell proliferation, colony formation, migration, and invasion [38]. miR-593 is upregulated in peritoneal lavage fluids of patients with pancreatic cancer. Upregulated miR-593 expression is significantly correlated with poor overall survival [39]. In contrast, miR-593 is downregulated in human hepatocellular carcinoma (HCC). The upregulation of miR-593 markedly decreases the proliferation, migration, and invasion of HCC cells [40]. Similarly, miR-593 inhibits the tumorigenesis of non-small cell lung cancer cells by targeting ICAM1 or PLK1 [41,42]. In this study, miR-593 mimics was found to markedly promote OS cell proliferation and migration (Figure 8B,C). This indicates that miR-593 suppression can be an alternative therapeutic approach for OS.

Meanwhile, the expression levels of *PRNP* and *HILPDA*, which

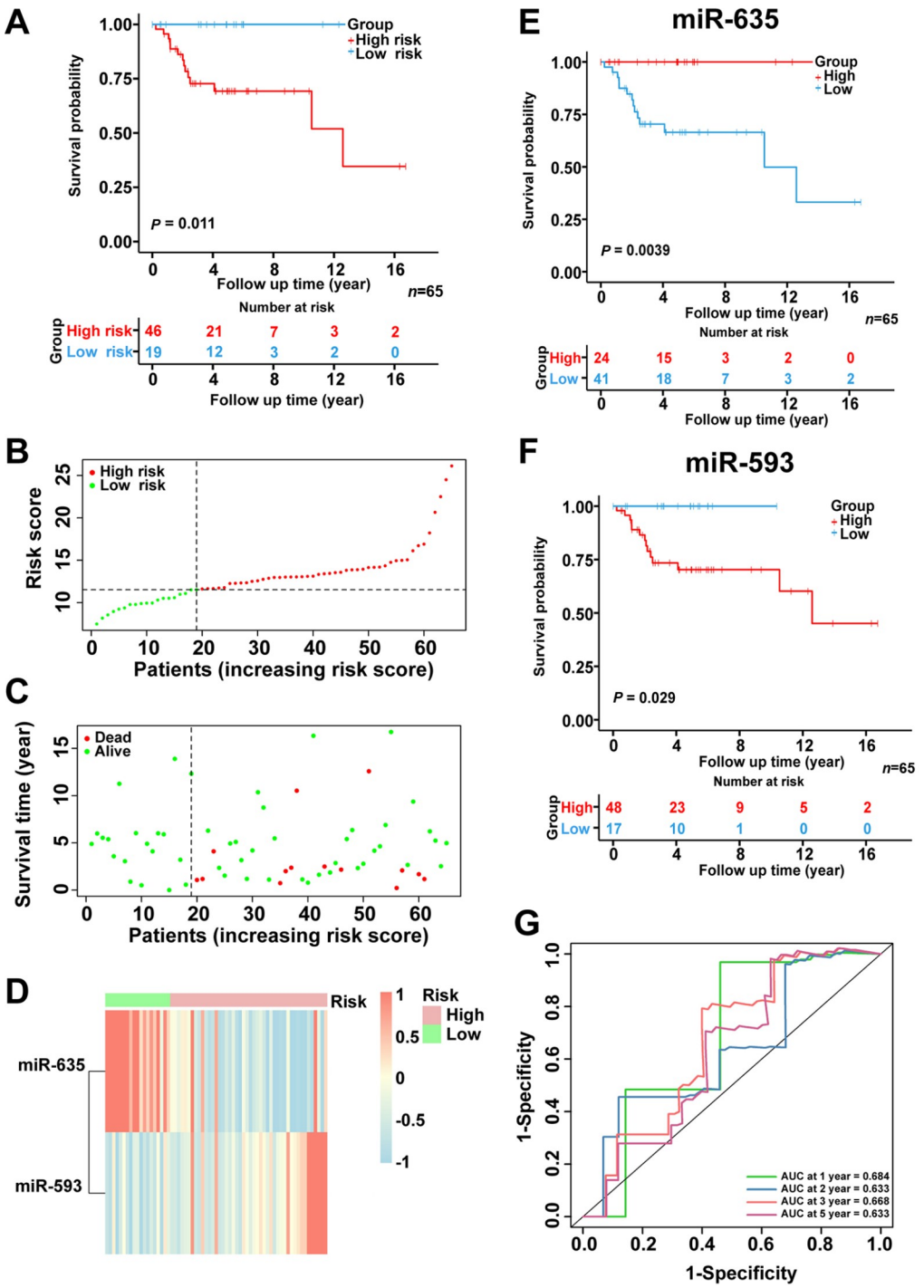


Figure 7. Validation of the prognostic signature in an external cohort (A) KM survival curves of patients in the two risk groups. (B) Distribution of patients with low and high risk scores in the validation cohort. (C) Distribution of overall survival status of patients with low and high risk scores in the validation cohort. (D) Differential expression of two FR_miRNAs between the low-risk and high-risk groups. (E) KM survival curve of patients according to miR-635 expression. (F) KM survival curve of patients according to miR-593 expression. (G) Evaluation of the same signature in a validation cohort based on the area under the receiver operating characteristic curve values for the 1-year, 2-year, 3-year, and 5-year survival rates.

are miR-635-associated and miR-593-associated FRGs, respectively, were significantly different between the low-risk and high-risk groups (Figure 6A,B). PRNP expression was reported to be negatively correlated with esophageal squamous cell carcinoma progression [43]. Ghazi *et al.* [44] reported that PRNP upregulation is a risk factor for patients with mesenchymal colorectal cancer, which indicates that the prognostic value of PRNP varies with the cancer type. miR-635 expression is positively correlated with *PRNP* expression (correlation index = 0.476 in Table 1). However, further experiments are needed to confirm this correlation. The expression

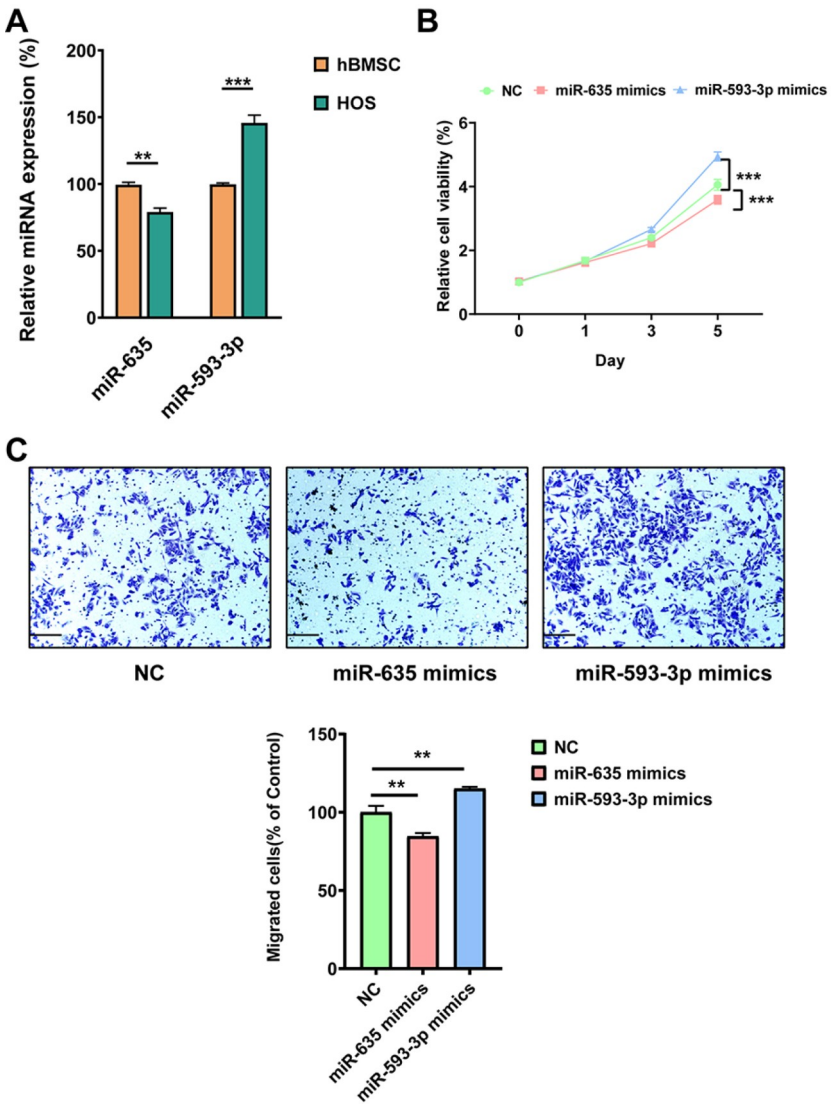


Figure 8. The expression of FR_miRNAs and its effect on the viability and migration of BMSCs and HOS cells (A) Compared with those in BMSCs, miR-635 was downregulated and miR-593 was upregulated in HOS cells. (B,C) OS cell viability and migration were upregulated upon transfection with miR-593 mimics but downregulated upon transfection with miR-635 overexpression construct (Scale bar: 150 μm).

of HILPDA is upregulated in most tumor types and is correlated with poor survival [45–47]. The prognostic model based on FRGs and/or miRNAs developed for various kinds of cancer exhibited good performance in predicting the prognosis of patients with cancer [48–51].

To the best of our knowledge, this is the first study to incorporate the ferroptosis process and its related miRNAs to construct a reliable tool for predicting the prognosis of patients with OS. Nevertheless, there are still some limitations in this study. The sample size in the study was small, which can be attributed to the low incidence of OS. Thus, oncologists encounter a limited number of patients with OS who consent to undergo gene testing. Studies on miRNAs have increased in the last decade. However, some miRNAs may have not yet been detected. The interaction of miRNAs with target FRGs was not examined in this study. Thus, the miRNAs included in this study may not be sufficient. Finally, the correlation between FRGs and miRNAs was not analyzed in the validated cohort, as the miRNA sequencing data were not sufficient for validation.

In conclusion, this study identified two FR_ miRNAs (miR-635 and miR-593) with contrasting roles in regulating OS cell proliferation and migration. A nomogram encompassing the FR_miRNA-based risk score and metastatic status was constructed to predict the prognosis of patients with OS. miR-635 and miR-593 might be therapeutic targets for OS treatment.

Supplementary Data

Supplementary data is available at *Acta Biochimica et Biophysica Sinica* online.

Funding

This work was supported by the grant from the Natural Science Foundation of Shanghai (No. 22ZR1476600).

Conflict of Interest

The authors declare that they have no conflict of interest.

References

1. Mutsaers AJ, Walkley CR. Cells of origin in osteosarcoma: mesenchymal stem cells or osteoblast committed cells? *Bone* 2014, 62: 56–63
2. Kansara M, Teng MW, Smyth MJ, Thomas DM. Translational biology of osteosarcoma. *Nat Rev Cancer* 2014, 14: 722–735
3. Bielack SS, Kempf-Bielack B, Delling G, Exner GU, Flege S, Helmke K, Kotz R, *et al.* Prognostic factors in high-grade osteosarcoma of the extremities or trunk: an analysis of 1,702 patients treated on neoadjuvant cooperative osteosarcoma study group protocols. *J Clin Oncol* 2002, 20: 776–790
4. Gianferante DM, Mirabello L, Savage SA. Germline and somatic genetics of osteosarcoma–connecting aetiology, biology and therapy. *Nat Rev Endocrinol* 2017, 13: 480–491
5. Szymanska J, Mandahl N, Mertens F, Tarkkanen M, Karaharju E, Knuutila S. Ring chromosomes in parosteal osteosarcoma contain sequences from 12q13-15: a combined cytogenetic and comparative genomic hybridization study. *Genes, chromosomes & cancer* 1996, 16: 31–34
6. Chen X, Kang R, Kroemer G, Tang D. Broadening horizons: the role of ferroptosis in cancer. *Nat Rev Clin Oncol* 2021, 18: 280–296
7. Dixon SJ, Lemberg KM, Lamprecht MR, Skouta R, Zaitsev EM, Gleason CE, Patel DN, *et al.* Ferroptosis: an iron-dependent form of nonapoptotic cell death. *Cell* 2012, 149: 1060–1072
8. Lin H, Chen X, Zhang C, Yang T, Deng Z, Song Y, Huang L, *et al.* EF24 induces ferroptosis in osteosarcoma cells through HMOX1. *BioMed Pharmacother* 2021, 136: 111202
9. Yang J, Zhou Y, Xie S, Wang J, Li Z, Chen L, Mao M, *et al.* Metformin induces ferroptosis by inhibiting UFMylation of SLC7A11 in breast cancer. *J Exp Clin Cancer Res*: CR 2021, 40: 206
10. Lei T, Qian H, Lei P, Hu Y. Ferroptosis-related gene signature associates with immunity and predicts prognosis accurately in patients with osteosarcoma. *Cancer Sci* 2021, 112: 4785–4798
11. Zhao J, Zhao Y, Ma X, Feng H, Jia L. Outstanding prognostic value of novel ferroptosis-related genes in chemoresistance osteosarcoma patients. *Sci Rep* 2022, 12: 5029
12. Shi Y, Gong M, Deng Z, Liu H, Chang Y, Yang Z, Cai L. Tirapazamine suppress osteosarcoma cells in part through SLC7A11 mediated ferroptosis. *Biochem Biophys Res Commun* 2021, 567: 118–124
13. Winkle M, El-Daly SM, Fabbri M. Noncoding RNA therapeutics-challenges and potential solutions. *Nat Rev Drug Discov* 2021, 20: 629–651
14. Rupaimoole R, Slack FJ. MicroRNA therapeutics: towards a new era for the management of cancer and other diseases. *Nat Rev Drug Discov* 2017, 16: 203–222
15. Bartel DP. MicroRNAs. *Cell* 2004, 116: 281–297
16. Wang JY, Yang Y, Ma Y, Wang F, Xue A, Zhu J, Yang H, *et al.* Potential regulatory role of lncRNA-miRNA-mRNA axis in osteosarcoma. *BioMed Pharmacother* 2020, 121: 109627
17. Soghli N, Ferns GA, Sadeghsoltani F, Qujeq D, Yousefi T, Vaghari-Tabari M. MicroRNAs and osteosarcoma: Potential targets for inhibiting metastasis and increasing chemosensitivity. *Biochem pharmacol* 2022, 201: 115094
18. Zhang H, Deng T, Liu R, Ning T, Yang H, Liu D, Zhang Q, *et al.* CAF secreted miR-522 suppresses ferroptosis and promotes acquired chemoresistance in gastric cancer. *Mol Cancer* 2020, 19: 43
19. Zhang GZ, Wu ZL, Li CY, Ren EH, Yuan WH, Deng YJ, Xie QQ. Development of a machine learning-based autophagy-related lncRNA signature to improve prognosis prediction in osteosarcoma patients. *Front Mol Biosci* 2021, 8: 615084
20. Wang B, Xiao H, Yang X, Zeng Y, Zhang Z, Yang R, Chen H, *et al.* A novel immune-related microRNA signature for prognosis of thymoma. *Aging* 2022, 14: 4739–4754
21. Ma B, Li H, Qiao J, Meng T, Yu R. Immune-related miRNA signature identifies prognosis and immune landscape in head and neck squamous cell carcinomas. *Biosci Rep* 2020, 40: BSR20201820
22. Zhang C, Liu X, Jin S, Chen Y, Guo R. Ferroptosis in cancer therapy: a novel approach to reversing drug resistance. *Mol Cancer* 2022, 21: 47
23. Sabharwal SS, Schumacker PT. Mitochondrial ROS in cancer: initiators, amplifiers or an Achilles' heel? *Nat Rev Cancer* 2014, 14: 709–721
24. Yang WS, SriRamaratnam R, Welsch ME, Shimada K, Skouta R, Viswanathan VS, Cheah JH, *et al.* Regulation of ferroptotic cancer cell death by GPX4. *Cell* 2014, 156: 317–331
25. Grignani G, Palmerini E, Ferraresi V, D'Ambrosio L, Bertulli R, Asaftei SD, Tamburini A, *et al.* Sorafenib and everolimus for patients with unresectable high-grade osteosarcoma progressing after standard treatment: a non-randomised phase 2 clinical trial. *Lancet Oncol* 2015, 16: 98–107
26. Ling H, Fabbri M, Calin GA. MicroRNAs and other non-coding RNAs as targets for anticancer drug development. *Nat Rev Drug Discov* 2013, 12: 847–865
27. Peng Y, Croce CM. The role of microRNAs in human cancer. *Sig Transduct Target Ther* 2016, 1: 15004
28. Rupaimoole R, Calin GA, Lopez-Berestein G, Sood AK. miRNA deregulation in cancer cells and the tumor microenvironment. *Cancer Discov* 2016, 6: 235–246
29. Gironella M, Seux M, Xie MJ, Cano C, Tomasini R, Gommeaux J, Garcia S, *et al.* Tumor protein 53-induced nuclear protein 1 expression is repressed by miR-155, and its restoration inhibits pancreatic tumor development. *Proc Natl Acad Sci USA* 2007, 104: 16170–16175
30. O'Connell RM, Chaudhuri AA, Rao DS, Baltimore D. Inositol phosphatase SHIP1 is a primary target of miR-155. *Proc Natl Acad Sci USA* 2009, 106: 7113–7118
31. Babar IA, Cheng CJ, Booth CJ, Liang X, Weidhaas JB, Saltzman WM, Slack FJ. Nanoparticle-based therapy in an in vivo microRNA-155 (miR-155)-dependent mouse model of lymphoma. *Proc Natl Acad Sci USA* 2012, 109: E1695–1704
32. Tili E, Croce CM, Michaille JJ. *miR-155*: on the crosstalk between inflammation and cancer. *Int Rev Immunol* 2009, 28: 264–284
33. Calin GA, Cimmino A, Fabbri M, Ferracin M, Wojcik SE, Shimizu M, Taccioli C, *et al.* MiR-15a and miR-16-1 cluster functions in human leukemia. *Proc Natl Acad Sci USA* 2008, 105: 5166–5171
34. Pekarsky Y, Croce CM. Role of miR-15/16 in CLL. *Cell Death Differ* 2015, 22: 6–11
35. Zhang Y, Sun Z, Zhang Y, Fu T, Liu C, Liu Y, Lin Y. The microRNA-635 suppresses tumorigenesis in non-small cell lung cancer. *BioMed Pharmacother* 2016, 84: 1274–1281
36. Tian L, Guo Z, Wang H, Liu X. MicroRNA-635 inhibits the malignancy of osteosarcoma by inducing apoptosis. *Mol Med Rep* 2017, 16: 4829–4834
37. Yang T, Guo JP, Li F, Xiu C, Wang H, Duan XL. Long non-coding RNA-DUXAP8 regulates TOP2A in the growth and metastasis of osteosarcoma via microRNA-635. *Mol Med Rep* 2021, 24: 511
38. Huang Q, Peng L, Sun Y, Huang J, Han T, Li Y, Peng H. miR-593-3p promotes proliferation and invasion in prostate cancer cells by targeting ADIPOR1. *Onco Targets Ther* 2021, 14: 3729–3737
39. Hata T, Mizuma M, Masuda K, Chiba K, Ishida M, Ohtsuka H, Nakagawa K, *et al.* MicroRNA-593-3p expression in peritoneal lavage fluid as a prognostic marker for pancreatic cancer patients undergoing staging laparoscopy. *Ann Surg Oncol* 2021, 28: 2235–2245
40. Gong XY, Huang AL. Regulatory roles of miR-593 in the proliferation and invasion of human hepatic carcinoma. *Eur Rev Med Pharmacol Sci* 2020,

24: 6657–6664
41. Yan L, Zhang Y, Li K, Wang M, Li J, Qi Z, Wu J, *et al*. miR-593-5p inhibit cell proliferation by targeting PLK1 in non small cell lung cancer cells. *Pathol Res Pract* 2020, 216: 152786
42. Zhang HB, Shen B, Ma ZC, Xu YY, Lou YL, Chen M. MiR-593-5p inhibited proliferation and migration of lung adenocarcinoma by targeting ICAM-1. *Eur Rev Med Pharmacol Sci* 2020, 24: 4298–4305
43. Zhao M, Li M, Zheng Y, Hu Z, Liang J, Bi G, Bian Y, *et al*. Identification and analysis of a prognostic ferroptosis and iron-metabolism signature for esophageal squamous cell carcinoma. *J Cancer* 2022, 13: 1611–1622
44. Ghazi A, Le Corre D, Pilati C, Taieb J, Aparicio T, Didelot A, Dedhar S, *et al*. Prognostic value of the PrP^{C}-ILK-IDO1 axis in the mesenchymal colorectal cancer subtype. *Oncoimmunology* 2021, 10: 1940674
45. Ma M, Liu L, Shi R, Zhang J, Li X, Li X, Bai J, *et al*. Copy number alteration profiling facilitates differential diagnosis between ossifying fibroma and fibrous dysplasia of the jaws. *Int J Oral Sci* 2021, 13: 21
46. Liu C, Zhou X, Zeng H, Wu D, Liu L. HILPDA is a prognostic biomarker and correlates with macrophage infiltration in Pan-Cancer. *Front Oncol* 2021, 11: 597860
47. VandeKopple MJ, Wu J, Auer EN, Giaccia AJ, Denko NC, Papandreou I. HILPDA regulates lipid metabolism, lipid droplet abundance, and response to microenvironmental stress in solid tumors. *Mol Cancer Res* 2019, 17: 2089–2101
48. Liang J, Wang D, Lin H, Chen X, Yang H, Zheng Y, Li Y. A novel ferroptosis-related gene signature for overall survival prediction in patients with hepatocellular carcinoma. *Int J Biol Sci* 2020, 16: 2430–2441
49. Zhu L, Yang F, Wang L, Dong L, Huang Z, Wang G, Chen G, *et al*. Identification the ferroptosis-related gene signature in patients with esophageal adenocarcinoma. *Cancer Cell Int* 2021, 21: 124
50. Selven H, Andersen S, Pedersen MI, Lombardi APG, Busund LTR, Kilvær TK. High expression of miR-17-5p and miR-20a-5p predicts favorable disease-specific survival in stage I-III colon cancer. *Sci Rep* 2022, 12: 7080
51. Hong X, Wang G, Pei K, Mo C, Rong Z, Xu G. A novel prognostic model based on seven Necroptosis-Related miRNAs for predicting the overall survival of patients with lung adenocarcinoma. *Biomed Res Int* 2022, 2022: 3198590